Mechanistic Implications of a Linear Free-Energy Correlation of Rate Constants for the Reduction of Active- and Met-R2 Forms of *E. coli* Ribonucleotide Reductase with Eight Organic Radicals

A. Mark Dobbing,[†] Christopher D. Borman,[†] Mark B. Twitchett,[†] David N. Leese,[†] G. Arthur Salmon,[‡] and A. Geoffrey Sykes*,[†]

Contribution from the Department of Chemistry, The University of Newcastle, Newcastle upon Tyne, NE1 7RU, UK, and The University of Leeds, Cookridge Radiation Research Centre, Leeds, LS16 6PB, UK

Received September 20, 1999

Abstract: Cross-reaction rate constants k_{12} (22 °C) at pH 7.0 have been determined for the reduction of Fe^{III}_2 and tyrosyl-radical-containing active-R2 from *E. coli* ribonucleotide reductase with eight organic radicals (OR), e.g., $MV^{\bullet+}$ from methyl viologen. The more reactive OR's were generated in situ using pulse radiolysis (PR) techniques, and other OR's were generated by prior reduction of the parent with dithionite, followed by stopped-flow (SF) studies. In both procedures it was necessary to include consideration of doubly-reduced parent forms. Values of k_{12} are in the range 10^9 to 10^4 M^{-1} s^{-1} and reduction potentials E^o_1 for the OR vary from −0.446 to +0.194 V. Samples of *E. coli* active-R2 also have an Fe^{III}_2 met-R2 component (with no $Tyr^{\bullet}$), which in the present work was close to 40%. From separate experiments met-R2 gave similar k_{12} rate constants (on average 66% bigger) to those for active-R2, suggesting that reduction of the Fe^{III}_2 center is the common rate-limiting step. A single Marcus free-energy plot of log k_{12} − 0.5 log f vs $-E^o_1/0.059$ describes all the data, and the slope of 0.54 is in satisfactory agreement with the theoretical value of 0.50. It is concluded that the rate-limiting step involves electron transfer. In addition, the intercept at $-E^o_1/0.059 = 0$ is 5.94, where values of the reduction potential and self-exchange rate constant for met-R2 contribute to this value. To maintain electroneutrality at the ∼10 Å buried active site H^+ uptake is also required. For both e^- and H^+ transfer the conserved pathway Trp-48, Asp-237, His-118 to Fe_A is a possible candidate requiring further examination.

Introduction

Ribonucleotide reductase (RNR)[1−6] catalyzes the de novo synthesis of the four deoxyribonucleotide components of DNA. Of the three classes of RNR,[5] those containing an Fe^{III}_2 center are the best characterized/understood, and that from *E. coli* is the most extensively studied. It consists of two nonidentical protein components R1 ($M_r = 2 \times 85.5$ kDa) and R2 ($M_r = 2 \times 43.5$ kDa), each having two identical subunits (hence $\alpha_2\beta_2$).[7] Only 16 of the R2 residues are conserved within 12 known sequences. The tyrosyl radical ($Tyr^{\bullet}$) of active-R2 is a deprotonated phenolate form.[4] X-ray crystal structures of R1 and R2 from *E. coli* have been reported.[8,9] In the R2 case the structures determined are for the met-R2 and reduced R2 forms,[9,10]

$$\underset{\text{active-R2}}{Fe^{III}_2\cdots Tyr^{\bullet}} \xrightarrow{e^-} \underset{\text{met-R2}}{Fe^{III}_2\cdots(TyrH)} \xrightarrow{2e^-} \underset{\text{red-R2}}{Fe^{II}_2\cdots(TyrH)} \quad (1)$$

where protonation of the phenolate O-atom of the nonradical met and red-R2 forms is indicated. Met-R2 and active-R2 have a μ-oxo bridged Fe^{III}_2, but the μ-oxo is no longer present in red-R2, and proton uptake is again evident. Therefore in (1) three electrons and as many as three protons are taken up in the conversion of $Fe^{III}_2\cdots Tyr^{\bullet}$ to $Fe^{II}_2\cdots(TyrH)$ with maintenance of electroneutrality. Features of the met-R2 structure are the position of the Fe^{III}_2 and tyrosyl-radical-forming Tyr-122, which are buried and ∼10 Å from the protein surface. The μ-oxo coupled Fe^{III}_2 is close to Tyr-122, with Fe_A 5.3 Å from the phenolate O-atom. The Fe^{III}_2 stabilizes the $Tyr^{\bullet}$ radical, and the reduced Fe^{II}_2 state is required for regeneration of $Tyr^{\bullet}$.[11] The mechanism of redox interconversion of R2 forms in (1) is a subject of current interest.[12−16]

The aim in these studies was to determine rate constants k_{12} for cross reactions involving the reduction of active-R2 from *E. coli* with eight organic radicals (OR), Figure 1. The rate

[†] The University of Newcastle.
[‡] The University of Leeds.

(1) Sjöberg, B.-M. *Struct. Bonding* **1997**, *88*, 139−173.
(2) Gräslund, A.; Sahlin, M. *Annu. Rev. Biophys. Biomol. Struct.* **1996**, *25*, 259−286.
(3) Wallar, B. J.; Lipscomb, J. D. *Chem. Rev.* **1996**, *96*, 2625−2657.
(4) Andersson, K. K.; Gräslund, A. *Adv. Inorg. Chem.* **1995**, *43*, 359−408.
(5) Sjöberg, B.-M. *Structure* **1994**, *2*, 793.
(6) Fontecave, M.; Nordlund, R.; Eklund, H.; Reichard, P. *Adv. Enzymol.* **1992**, *65*, 147−183.
(7) Nilsson, O.; Lundqvist, T.; Hahne, S.; Sjöberg, B.-M. *Biochem. Soc. Trans.* **1988**, *16*, 91.
(8) Uhlin, U.; Eklund, H. *Nature (London)* **1994**, *70*, 533.
(9) Nordlund, P.; Eklund, H. *J. Mol. Biol.* **1993**, *232*, 123.
(10) Logan, D. T.; Su, X.-D.; Åberg, A.; Regnström, K.; Hajdu, J.; Eklund, H.; Nordlund, P. *Structure* **1996**, *4*, 1053.
(11) Ravi, N.; Bollinger, J. M., Jr.; Huynh, B. H.; Edmondson, D. E.; Stubbe, J. *J. Am. Chem. Soc.* **1994**, *116*, 8007.
(12) Han, J.-Y.; Gräslund, A.; Thelander, L.; Sykes, A. G. *J. Biol. Inorg. Chem.* **1997**, *2*, 287.
(13) Dobbing, A. M.; Han, J.-Y.; Sykes, A. G. *J. Biol. Inorg. Chem.* **1998**, *3*, 480.
(14) Han, J.-Y.; Swarts, J. C.; Sykes, A. G. *Inorg. Chem.* **1996**, *35*, 4629.
(15) Swarts, J. C.; Aquino M. A. S.; Han, J.-Y.; Lam, K.-Y.; Sykes, A. G. *Biochim. Biophys. Acta.* **1995**, *1247*, 215.
(16) Davydov, A.; Schmidt, P. P.; Gräslund, A. *Biochem. Biophys. Res. Commun.* **1996**, *219*, 213−218.

10.1021/ja993412k CCC: $19.00
Published on Web 02/29/2000

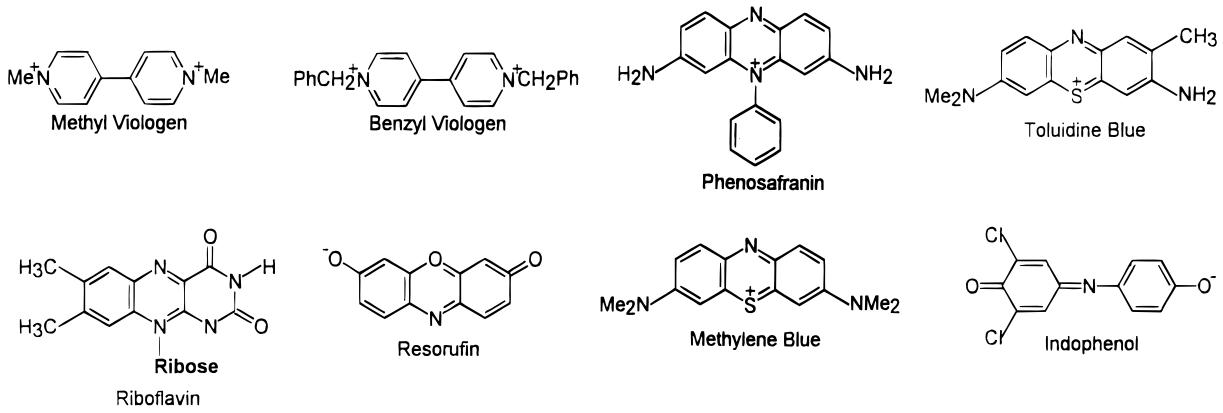

Figure 1. Formulas (pH ~7) of eight parent reagents (X) used to generate the organic radicals OR ($X^{\bullet -}$ in this study).

constants are appraised in terms of the Marcus equations for outer-sphere electron-transfer reactions

$$k_{12}^{\ 2} = k_{11}k_{22}K_{12}f \tag{2}$$

$$\log f = \frac{(\log K_{12})^2}{4\log(k_{11}k_{22}/Z^2)} \tag{3}$$

where k_{11} and k_{22} are self-exchange rate constants for the OR and relevant R2 couple (which we specify later), respectively, and the collision frequency Z is assumed to be $10^{11}M^{-1}\ s^{-1}$.[17] Using the Nernst equation the equilibration constant K_{12} for the cross reaction is given by $\log K_{12} = (E^o_2 - E^o_1)/0.059$, where E^o_1 and E^o_2 are reduction potentials in volts (vs NHE) applying to the OR and R2 couples, respectively. Equation 2 can be expressed in the alternative form

$$(\log k_{12} - 0.50\log f) = 0.50(\log k_{11} + \log k_{22} + E^o_2/0.059) - 0.50E^o_1/0.059 \tag{4}$$

To test for (4) the left-hand side is plotted against $-E^o_1/0.059$. Hence the free-energy dependence of $\Delta G^{\dagger}_{12}$ on ΔG^o_{12} is explored, or more precisely the E^o_1 term of ΔG^o_{12}. Active-R2 has an Fe^{III}_2 met-R2 component that has to be taken into account. No preparation to date has <25% of met-R2.[18] Rate constants (k_{12}) for the reaction of met-R2 were also determined by independent experiments, and are an important mechanistic contribution to the studies described.

The procedures used have been tested previously for the reduction of cytochrome *c*(III) with the same eight OR's,[19] where a plot of (4) has a slope of 0.49 (theoretical value 0.50) and intercept at $-E^o_1/0.059 = 0$ of 6.57. The latter was calculated as 6.55 from known parameters and assuming a common k_{11} of $1.0 \times 10^6\ M^{-1}\ s^{-1}$ for the self-exchange of the different OR's with the parent form.[20−22] It is possible therefore to proceed with this same value of k_{11} in the present studies, and comment on the magnitude of E^o_2 and k_{22} respectively for R2. The procedure initially devised to study these reactions,[23] is no longer appropriate since no account was taken of the direct reduction of R2 by excess dithionite,[13] which at the time was reported to be negligible.

Experimental Section

Protein Source. Wild-type *E. coli* R2 was prepared as the $\beta\beta$ protein from an *E. coli* overproducing strain,[24] kindly provided by Professor B.-M. Sjöberg, University of Stockholm, Sweden. Concentrated solutions of R2 (~0.3 mM), consisting of a mix of active-R2 (60%) and met-R2 (40%) forms, were stored in small batches at −80 °C. Protein was made air-free by dialyzing against deaerated buffer. Met-R2 was prepared by reacting the above R2 mix with hydroxyurea (50 mM) at 25 °C for ~30 min, after which excess hydroxyurea was removed using a Sephadex G-25 column or by dialysis. The dilute met-R2 solution was concentrated by ultra-dialysis against deaerated 50 mM Tris/HCl at pH 7.5 containing 20% glycerol.[25] The UV−vis spectra of active- and met-R2 allow the composition to be determined using known absorption coefficients (ϵ).[26] In the case of active R2 a sharp band at 410 nm (ϵ ~6600 $M^{-1}\ cm^{-1}$)[26] is largely due to $Tyr^{\bullet}$. The $Tyr^{\bullet}$ also has a weak absorbance at ~600 nm, which contributes to the characteristic green color of active R2. Fully reduced Fe^{II}_2 protein has little or no absorbance at >400 nm. Concentrations of protein were determined spectrophotometrically using the difference in absorption coefficients $\epsilon_{280} - \epsilon_{310} = 1.2 \times 10^5\ M^{-1}\ cm^{-1}$.[27]

Buffers. For kinetic experiments all solutions were made up to pH 7.0, I = 0.100 M, using sodium hydrogen phosphates (Sigma). During the preparation tris(hydroxymethyl)aminomethane (Tris; pH range 7.1−8.9) was used.

Reagents for Organic Radicals. The following parent forms, Figure 1, with trivial, systematic, and abbreviated names as indicated, were used to generate the one-electron reduced organic radicals (OR): methyl viologen, $C_{12}H_{14}N_2Cl_2$ (1,1′-dimethyl-4,4′-bipyridinium dichloride), MV^{2+}; benzyl viologen, $C_{24}H_{22}N_2Cl_2$ (1,1′-dibenzyl-4,4′-bipyridinium dichloride), BV^{2+}; phenosafranin, $C_{18}H_{15}N_4Cl$ (3,7-diamino-5-phenylphenazinium chloride), Pf^+; riboflavin $C_{17}H_{20}N_4O_6$ (vitamin B_2), Rb; resorufin, $C_{12}H_6NO_3Na$ (7-hydroxy-3*H*-phenoxazin-3-one sodium salt), Rf^-; methylene blue $C_{16}H_{18}N_3SCl$ (3,7-bis(dimethylamino)phenazothionium chloride), MB^+; toluidine blue, $(C_{15}H_6N_3SCl)_2{\cdot}ZnCl_2$ (approximate formula only), TB^+; and indo-phenol, $C_{12}H_6Cl_2NO_2Na$ (phenolindo-2,6-dichlorophenol sodium salt), IP^-. These were obtained from Sigma Chemicals, except MB^+ and IP^- (BDH), and TB^+ (Fluka). Toluidine Blue (1 g) was recrystallized by being dissolved in H_2O (18 mL) at 80 °C. Ethanol (13.5 mL) was added with stirring over ~10 min at 0 °C. The solid obtained was filtered off, washed with cold ether, and dried in a desiccator containing silica gel (yield 28%). Redox titration with

(17) Marcus, R. A.; Sutin, N. *Biochim. Biophys. Acta* **1985**, *811*, 265−322.
(18) Lynch, J. B.; Juarez-Garcia, C.; Münck, E.; Que, L., Jr. *J. Biol. Chem.* **1989**, *264*, 8091.
(19) Borman, C. D.; Dobbing, A. M.; Salmon, G. A.; Sykes, A. G. *J. Phys. Chem. B* **1999**, *103*, 6605.
(20) de Oliveira, L. A. A.; Haim, A. *J. Am. Chem. Soc.* **1982**, *104*, 3363.
(21) Curtis, J. C.; Sullivan, B. P.; Meyer, T. J. *Inorg. Chem.* **1980**, *19*, 3833.
(22) Tsukahara K.; Wilkins, R. G. *J. Am. Chem. Soc.* **1985**, *107*, 2632.
(23) Lam, K.-Y.; Fortier, D. G.; Sykes, A. G. *J. Chem. Soc., Chem. Commun.* **1990**, 1019.
(24) Sjöberg, B.-M.; Hahne, S.; Karlsson, M.; Jörnvall, H.; Goransson, M.; Uhlin, B. E. *J. Biol. Chem.* **1986**, *261*, 5658.
(25) Barlow, T.; Eliasson, R.; Platz, A.; Reichard, P.; Sjöberg, B.-M. *Proc. Natl. Acad. Sci. U.S.A.* **1983**, *80*, 1492.
(26) Petersson, L.; Gräslund, A.; Ehrenberg, A.; Sjöberg, B.-M.; Reichard, P. *J. Biol. Chem.* **1980**, *255*, 6706.
(27) Climent, I.; Sjöberg, B.-M.; Huang, C. Y. *Biochemistry* **1992**, *31*, 4801.

dithionite gave 81% reactivity in accordance with that expected from the formula $(C_{15}H_6N_3SCl)_2 \cdot ZnCl_2$, and was used in this work, see also ref 19. Some difficulties were encountered in dissolving resorufin, and solutions were prepared by sonicating appropriate mixes for 1 h and then filtering through a 2 μm Acrodisc filter (Gellman).

The parent forms MV^{2+} and BV^{2+} are colorless and the OR's have peaks λ/nm (ϵ/M^{-1} cm^{-1}) at 606 (12400) and 555 (11250), respectively.[28,29] All the other parent forms are colored with peak positions Pf^+ 521 (3.3×10^4), Rb 445 (1.1×10^4), Rf^- 570 (4.5×10^4), MB^+ 660 (7.8×10^4), TB^+ 632 (5.8×10^4), and IP^- 603 (1.4×10^4). Methylene Blue has been fairly extensively studied and the radical $MB^\bullet$ shown to disproportionate $2MB^\bullet \rightleftarrows MB^- + MB^+$ with $K \sim 2 \times 10^5$. The rate constant for the forward reaction is in the range $(1.5-3.0) \times 10^9 M^{-1}s^{-1}$.[30] Double reduction of parent forms (with $S_2O_4^{2-}$) and/or formation of the double reduced form by disproportionation of OR has to be considered in this work.

Electrochemistry. Reduction potentials (E^o_1 vs NHE) for the parent/OR couples were checked by cyclic voltammetry (CV) using a Princeton Applied Research model 173 potentiostat, as previously described.[19] In all but two cases these were within 10 mV of literature values,[31] see listing in Table 5. One exception is with Toluidine Blue, for which a value of 0.015 V, as compared to a literature value of 0.034 V,[32] has been obtained. The other is with Indo-Phenol for which a 22 mV smaller value is obtained.

Procedures for Pulse Radiolysis Studies. Experiments were carried out on a Van de Graaff accelerator at the Cookridge Radiation Research Centre, University of Leeds, using a triple-pass cell (6.9 cm light path length) and a 2.5 MeV ($\sim 4 \times 10^{-16}$ J) beam of electrons.[33] Pulse lengths were 0.6 μs, and under the conditions adopted the production of radicals by each pulse was as in

$$4.23H_2O \rightarrow e^-_{aq}\ (2.8),\ OH^\bullet\ (2.8),\ H^\bullet\ (0.62),\ H^+\ (2.8),\ H_2O_2\ (0.73) \quad (5)$$

where 10^7 G values in brackets correspond to the number of moles of product per joule of energy absorbed.[33] Solutions for kinetic studies were at pH 7.0 (40.5 mM phosphate), contained 0.010 M sodium formate, and were saturated with N_2O, $I = 0.100$ M. Subsequent reactions are

$$e^-_{aq} + N_2O + H_2O \rightarrow N_2 + OH^- + OH^\bullet \quad (6)$$

$$OH^\bullet/H^\bullet + HCO_2^- \rightarrow CO_2^{\bullet-} + H_2O/H_2 \quad (7)$$

$$CO_2^{\bullet-} + X \rightarrow CO_2 + X^{\bullet-} \quad (8)$$

where in the present case $X^{\bullet-}$ is the OR and X the parent. A large excess of X ($\sim 1.0 \times 10^{-4}$M) was used so that the formate radical $CO_2^{\bullet-}$ is effectively scavenged, generating $X^{\bullet-}$ as the only reducing species present in solution. With such a choice of reactant concentrations double reduction of the parent is precluded. The addition of $2X^{\bullet-}$ to X_2^{2-} or disproportionation to X and X^{2-} also needs to be considered. Experiments were at temperatures in the range 22 ± 1 °C.

Samples of R2 (~ 100 μM) were dialyzed against two portions of deaerated buffer (each ≥ 200 times the volume of R2 solution) and stored under N_2 before use. Prior to each experiment buffer solutions containing 100 μM of the parent X (~ 10 mL) were saturated with N_2O and argon by bubbling for at least 20 min. Calculated amounts of stock deaerated protein were added to give the required concentration (~ 10 μM). Gastight syringes were essential when loading the sample cell, and a positive pressure of argon was maintained while loading and draining the cell.

Reactions with R2 were monitored at the peak positions λ/nm for the OR's as follows: $MV^{\bullet+}$ (606), $BV^{\bullet+}$ (555), $Pf^\bullet$ (670), $Rb^{\bullet-}$ (550 and 600), and $Rf^{\bullet 2-}$ (700). At these wavelengths absorption by the radical is large and absorption by the protein and parent forms is relatively small. Rate constants reported are average values using 3−4 fresh amounts of the same reactant solutions.

Stoichiometries for Parent Forms with Dithionite. In the stopped-flow studies prior reduction of parent MB^+, TB^+, and IP^- forms with dithionite is required.[19] The stoichiometries were determined by addition of ~ 2 mM sodium dithionite in air-free conditions (glovebox, $O_2 < 3$ ppm) until only a trace of color remained.[19] Dithionite is a two-equivalent reducing agent $S_2O_4^{2-} - 2e^- \rightarrow 2SO_2$ (i.e. SO_3^{2-}). The number of moles of dithionite required for bleaching of the parent was 0.98 for MB^+ and 0.96 for TB^+, and 0.47 mol in the case of the quinone type molecule IP^-. In the first two instances therefore double reduction and in the latter single reduction of the parent is observed.

Procedure for Stopped-Flow Studies. An Applied Photophysics UV−vis stopped-flow spectrophotometer was used to monitor reactions. Rigorous air-free conditions were achieved by replacing connecting leads on the stopped-flow by polyetheretherketone (PEEK) tubing which has low O_2 permeability, and by prior bubbling of N_2 through all but R2 solutions which were stored long-term under N_2. The flow system was washed with dithionite immediately prior to use. Reduction of the three parent forms MB^+, TB^+, and IP^- was by dropwise addition of concentrated (~ 10 mM) sodium dithionite using a Gilson pipetman in a glovebox ($O_2 < 3$ ppm) until there was little color remaining. An excess of dithionite was avoided because of possible contributions from direct reduction of active- and met-R2.[13] Reactant concentrations used were in the range 4.1−9.9 μM for parent and 30−47 μM for R2. Conditions were 22.0 ± 0.1 °C, pH 7.0 (45 mM phosphate), $I = 0.100 \pm 0.002$ M. Reactions were monitored at peak positions for reformation of the parent forms λ/nm ($\epsilon/M^{-1}cm^{-1}$): MB^+ 660 (7.4×10^4), TB^+ 632 (5.8×10^4), and IP^- 603 (1.4×10^4). At wavelengths >600 nm absorption coefficients for active- and met-R2 are <600 $M^{-1}cm^{-1}$. The reactivities with TB^+ and IP^- were also monitored at the 410 nm R2 peak. At 410 nm, $MB^\bullet$ absorbs strongly.[30] Stopped-flow-loaded reactant solutions were repeat triggered 4 times and averaging procedures carried out.

Treatment of Data. In pulse radiolysis studies the program FACSIMILE[34] was used to fit UV−vis absorbance−time data. In the stopped-flow studies the Applied Photophysics global analysis program Glint (version 4.10) was used.

Results

Initial Studies of R2 with $CO_2^{\bullet-}$ and e^-_{aq}. A solution of R2 (7.3μM) at pH 7.0 (40.5 mM phosphate), 0.010 M formate, $I = 0.100$ M, was subjected to a dose of 1 Gy of radiation, which gave 0.60 μM $CO_2^{\bullet-}$ (reduction potential −1.9 V). No reaction was observed at 410 nm over 10 μs to 10 s at 22 ± 1 °C. At 350 nm rapid formation and decay of $CO_2^{\bullet-}$ could be monitored ($\epsilon = 250$ M^{-1} cm^{-1}) with rate constant $2k(CO_2^{\bullet-} + CO_2^{\bullet-}) = 1.0 \times 10^9$ M^{-1} s^{-1} for the decay process. On repeating with no phosphate or protein present a rate constant of 0.91×10^9 M^{-1} s^{-1} was obtained as compared to a literature value of 1.3×10^9 M^{-1} s^{-1}.[35]

To generate e^-_{aq} (−2.9 V) a solution of R2 (5.1 μM) at pH 7.0 (45 mM phosphate) containing *tert*-butyl alcohol (50 mM), $I = 0.100$ M, was subjected to a dose of 1 Gy of radiation, which gave 0.30 μM of e^-_{aq}. At the 410 nm R2 peak no reaction was observed over 10 μs to 10 s. Decay of the e^-_{aq} absorbance at 650 nm ($\epsilon = 16.8 \times 10^3$ M^{-1} cm^{-1})[33] was approximately first order with a rate constant of $5.2 \times 10^5 s^{-1}$. This can be largely accounted for by the reaction of e^-_{aq} with phosphate buffer. The rate constant for the reaction of e^-_{aq} with R2 would

(28) Zare, R. N. *Ber. Bunsen-Ges. Chem.* **1974**, *78*, 153.
(29) Bird, C. L.; Kuhn, A. T. *Chem. Soc. Rev.* **1981**, *10*, 49−82.
(30) Keene, J. P.; Land, E. J.; Swallow, A. J., Ed. Baxendale J.H Academic Press: London, 1965; p 225.
(31) Clark, W. M. *Oxidation and Reduction Potentials of Organic Systems*; Williams and Wilkins: Baltimore, Maryland, 1960.
(32) Steihler, R. D.; Chen, T.-T.; Clark, W. M. *J. Am. Chem. Soc.* **1933**, *55*, 891.
(33) Salmon, G. A.; Sykes, A. G. *Methods Enzymol.* **1993**, *227*, 522.
(34) Curtis, A. R.; Sweetenham, W. P. FACSIMILE/CHECKMAT Users Manual, UKAEA, Atomic Energy Research Establishment, Harwell, 1987, R12805.
(35) Sellers, R. M. Ph.D. Thesis, University of Leeds, 1972.

have to be $>2 \times 10^{10}$ M^{-1} s^{-1} to contribute >20% to the changes observed.

It is concluded that there is no measurable reaction of $CO_2^{\bullet-}$ or e^-_{aq} with active- or met-R2.

Rate Constants for the Disproportionation of OR's. Rate constants k_D(22 °C) for the disproportionation of OR (here $X^{\bullet-}$)

$$2X^{\bullet-} \rightarrow X + X^{2-} \text{ (or } X_2^{2-}) \qquad (9)$$

where X is the parent form, were determined by monitoring the absorbance decay at the OR peak positions $Pf^{\bullet}$ (670 nm), $Rb^{\bullet-}$ (600 nm), and $Rf^{\bullet 2-}$ (700 nm). The PR dose gave OR concentrations of ~0.6 μM. Parent concentrations were 100 μM, pH 7.0 (40.5 mM phosphate buffer), with 0.010 M sodium formate present, $I = 0.100$ M. Rate constants k_D/M^{-1} s^{-1} obtained were $4.4(8) \times 10^9$ ($Pf^{\bullet}$), $1.9(8) \times 10^9$ ($Rb^{\bullet-}$), and $3.0(3) \times 10^8$ ($Rf^{\bullet 2-}$). Flash photolysis studies involving $Rb^{\bullet-}$ disproportionation have previously been reported.[35] The radical $MV^{\bullet+}$ is long-lived and reaction 9 does not occur. With $BV^{\bullet+}$ dimerization rather than disproportionation occurs,[36,37] but is negligible for the concentrations used in these studies.

Reactions of OR's with R2 by Pulse Radiolysis. Absorption changes were monitored at wavelengths for decay of the OR's (see Experimental Section). At these wavelengths absorptions of the parent and R2 forms are small. The rate constant k_0 for (10) is $>5 \times 10^9$ M^{-1} s^{-1},

$$CO_2^{\bullet-} + X \xrightarrow{k_0} CO_2 + X^{\bullet-} \qquad (10)$$

and is rapid compared to other steps (eqs 11−13).

$$X^{\bullet-} + Fe^{III}{}_2\cdots Tyr^{\bullet} \xrightarrow{k_1} X + Fe^{II}Fe^{III}\cdots Tyr^{\bullet} \qquad (11)$$

$$X^{\bullet-} + Fe^{III}{}_2 \xrightarrow{k_2} Fe^{II}Fe^{III} + X \qquad (12)$$

$$2X^{\bullet-} \xrightarrow{k_D} X_2^{2-} \text{ or } X + X^{2-} \qquad (13)$$

Satisfactory fits to absorbance vs time data were obtained using the FACSIMILE program.[34] Solutions of met-R2 allowed k_2 in (12) to be determined by separate experiment. Solutions of active-R2 have a met-R2 component (~40%), and concurrent reactions have to be considered. In the case of the $MV^{\bullet+}$ and $BV^{\bullet+}$ (11) and (12) are favorable compared to (13),[37,38] and k_1 and k_2 were obtained from first-order decay processes. For $Pf^{\bullet}$, $Rb^{\bullet-}$, and $Rf^{\bullet 2-}$, k_1, k_2, and k_D are relevant, where k_D and k_2 are as determined in separate experiments. Examples of fits of data are shown for $Pf^{\bullet}$ in Figure 2 and for $Rb^{\bullet-}$ and Rf^{2-} as Supporting Information. No further steps corresponding to the further reaction of X^{2-} were required in the fitting process. Values of k_1 and k_2 are listed in Table 1. The similarity of k_1 and k_2 values ($k_2 > k_1$ by an average 66%) implies an identical redox step $Fe^{III}{}_2 \rightarrow Fe^{II}Fe^{III}$. This is an unexpected result in view of the reduction potential for the $Tyr^{\bullet}$/Tyr couple currently believed to be ~1.0 V.[39] Details of the $Fe^{II}Fe^{III}$ decay have not been established, but the reaction is known to be rapid from EPR freeze-quench experiments.[40,41] In Table 2, ϵ values for $Pf^{\bullet}$, $Rb^{\bullet}$, and $Rf^{\bullet 2-}$, and for $Fe^{II}Fe^{III}$ obtained as part of the fitting procedure, are listed. The ϵ values for $Fe^{II}Fe^{III}$ are small compared to those for the OR's. No major peak positions in the 550−700 nm range were indicated, and further details were not explored as a part of these studies. The reaction of $MB^{\bullet}$ was also studied by PR, but rates are too slow and the fit is less precise than when the SF method is used.

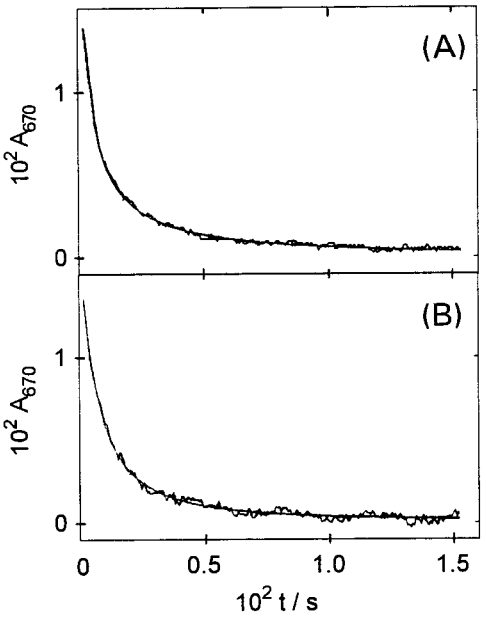

Figure 2. Fit of absorbance−time data from pulse radiolysis studies to eqs 11−13 (as appropriate) for reactions of the radical $Pf^{\bullet}$ (100 μM) with *E. coli* R2 monitored at 670 nm: (A) the reaction of met-R2 (10 μM) and (B) the reaction of active-R2 (10 μM, 40% of which is met-R2), using the FACSIMILE program. Conditions: 22 °C, pH 7.0 (40.5 mM phosphate), $I = 0.100$ M.

Table 1. Results from Pulse Radiolysis Experiments[a]

OR	$k_1/M^{-1}\,s^{-1}$ [b]	$k_2/M^{-1}\,s^{-1}$ [c]
$MV^{\bullet+}$	$1.06(2) \times 10^9$	$2.00(2) \times 10^9$
$BV^{\bullet+}$	$3.3(4) \times 10^8$	$3.5(2) \times 10^8$
$Pf^{\bullet}$	$2.2(4) \times 10^7$	$3.4(5) \times 10^7$
$Rb^{\bullet-}$	$1.1(1) \times 10^7$	$2.6(2) \times 10^7$
$Rf^{\bullet 2-}$	$2.7(5) \times 10^6$	$3.4(5) \times 10^6$

[a] Rate constants (22 °C) for reactions of active-R2 (k_1) and met-R2 (k_2) with organic radicals (OR), pH 7.0 (40.5 mM phosphate), $I = 0.100$ M. [b] Listed as k_{12} for active-R2 in Table 5. [c] Listed as k_{12} for met-R2 in Table 5.

Table 2. Absorption Coefficients (ϵ) for the Parent, Organic Radical (OR), and $Fe^{II}Fe^{III}$ (R2) Intermediate (not previously determined) from Pulse Radiolysis Experiments, Using the FACSIMILE Program and Monitoring the Decay of the UV−Vis Absorbance of the OR (wavelength indicated)[a]

OR	λ/ nm	ϵ(parent)/ $M^{-1}\,cm^{-1}$	ϵ(OR)/ $M^{-1}\,cm^{-1}$	$\epsilon(Fe^{II}Fe^{III})$/ $M^{-1}\,cm^{-1}$
Pf	670	950(80)	10440(300)	1310(150)
$Rb^{\bullet-}$	550	~10	5390(240)	1500(100)
	600	~10	3730(90)	1090(30)
$Rf^{\bullet 2-}$	700	400(60)	3550(260)	1010(100)

[a] pH 7.0 (40.5 mM phosphate), $I = 0.100$ M.

Reactions of OR's with R2 by Stopped-Flow. The dithionite procedure for the reduction of the parent X gives double-reduced X^{2-} forms of MB^+ and TB^+, and single reduced $X^{\bullet-}$ in the

(36) Ahmed, I.; Cusanovich, M. A.; Tollin, G. *Proc. Natl. Acad. Sci. U.S.A.* **1981**, *78*, 6724.
(37) Van Leeuwen, J. W.; van Dijk, C.; Veeger, C. *Eur. J. Biochem.* **1983**, *135*, 601.
(38) Carey, J. G.; Cairns, J. F.; Colchester, J. E. *J. Chem. Soc., Chem. Commun.* **1969**, 1280.
(39) Silva, K. E.; Elgren, T. E.; Que, L., Jr.; Stankovich, M. T. *Biochemistry* **1995**, *34*, 14093.
(40) Atta, M.; Anderson, K. K.; Ingemarson, R.; Thelander, L.; Gräslund, A. *J. Am. Chem. Soc.* **1994**, *116*, 6429.
(41) Gerez, C.; Fontecave, M. *Biochemistry* **1992**, *31*, 780.

Table 3. Stopped-Flow Studies (22 °C) on the Reduction of the Active-R2 Component $Fe^{III}_2\cdots Tyr^{\bullet}$ (46.7 μM) with Toluidine Blue (4.4 μM)[a]

$10^{-9}k_D$(start)	$10^{-5}k_1$[b]	$10^{-5}k_3$	$10^{-9}k_D$(final)
0.01	37(6)	3.2(7)	0.057(6)
0.30	7.1(3)	5.6(2)	1.2(3)
1.5[c]	6.9(3)	5.7(2)	1.5[d]

[a] pH 7.0 (45 mM phosphate), $I = 0.100$ M, monitored at 632 nm. Solutions of the parent X were reduced with dithionite prior to stopped-flow mixing. The program Glint was used to fit rate constants k_1 (reaction of $X^{\bullet-}$) and k_3 (reaction of X^{2-}), using different starting values for k_D (examples given). A best fit value for k_D is indicated. [b] Listed as k_{12} in Table 5. [c] Best fit k_D. [d] Does not vary during fit.

case of IP^-. Experiments on the reaction of dithionite reduced MB^+ and IP^- (2.8μM) with met-R2 (17.5μM) were explored (under N_2) using a two compartment (split) optical cell. The latter (total solution volume 2.6 mL) was loaded and initial absorbance readings taken prior to mixing. No reaction was observed over >2 h indicating a reduction potential for the met-R2 $Fe^{III}_2/Fe^{III}Fe^{II}$ couple of <0.011 V. This value is in keeping with the two-equivalent reduction potential of −0.115 V for the Fe^{III}_2/Fe^{II}_2 couple.[39] In the case of mouse R2 the reduction potential for the $Fe^{III}_2/Fe^{II}Fe^{III}$ couple has been estimated as 0.150 to 0.010 V,[40] and if such a range holds also for *E. coli* met-R2 then it is expected that some of the OR radicals will have difficulty in bringing about reduction of met-R2. Reactions with active-R2 could, however, be studied because the unfavorable reduction of $Fe^{III}_2\cdots Tyr^{\bullet}$ to $Fe^{II}Fe^{III}\cdots Tyr^{\bullet}$ is followed by the favorable intramolecular redox change to give met-R2.

The reaction scheme to be considered is therefore

$$X^{2-} + Fe^{III}_2\cdots Tyr^{\bullet} \xrightarrow{k_3} X^{\bullet-} + Fe^{II}Fe^{III}\cdots Tyr^{\bullet} \quad (14)$$

$$2X^{\bullet-} \xrightarrow{k_D} X^{2-} + X \quad (15)$$

$$X^{\bullet-} + Fe^{III}_2\cdots Tyr^{\bullet} \xrightarrow{k_1} Fe^{II}Fe^{III}\cdots Tyr^{\bullet} \quad (16)$$

Concentrations of the parent were in the range 4.1−9.9 μM, and of active-R2 in the range 30−47 μM. A fitting procedure for toluidine blue was employed using absorbance−time data at 632 nm, and the Glint program with different k_D(start) values. As can be seen from Table 3, k_1 and k_3 converge and give a k_D(final) value of 1.5×10^9 M^{-1} s^{-1} after a number of iterations. The same k_D was used for methylene blue, where values of k_D in the range $(1.5-3.0) \times 10^9$ M^{-1} s^{-1} have been determined previously.[30] No double reduction is observed with indo-phenol and a simpler treatment was possible. The TB^+ reaction was also monitored at 410 nm. The latter is an absorbance peak for $Tyr^{\bullet}$ with smaller absorbance contributions from Fe^{III}_2.[26] As can be seen from Table 4 identical rate constants are obtained at both wavelengths. The absorbance change at 410 nm was 0.016, which is bigger than the absorbance change for $Fe^{III}_2 \rightarrow Fe^{II}_2$ (0.009). On this evidence reduction of the $Tyr^{\bullet}$ occurs rapidly and within the first phase of reaction. The IP^- reaction was also monitored at 410 nm, Table 4. Since $MB^{\bullet}$ absorbs strongly at 410 nm, no similar studies were possible. Values of k_1 are listed in Table 5 as k_{12}.

Free-Energy Plot. Rate constants (k_{12}) at pH 7.0 for the eight OR reactions with active-R2 and for five OR reactions with met-R2 are listed in Table 5. In those cases in which both have been studied the met-R2 rate constant is the larger, but only by a small amount (average ∼66%). This is most likely due to minor structural differences at the active site. A graph of log $k_{12} - 0.5 \log f$ against $-E^o_1/0.059$, Figure 4, gives a single line for all the data of slope 0.54(2) in satisfactory agreement with the theoretical value of 0.50, and an intercept of 5.94(9) equal to 0.50 ($\log k_{11} + \log k_{22} + E^o_2/0.059$). Separate consideration of the active-R2 points has negligible (∼2%) effect on slope and intercept values. Assuming E^o_2 for the *E. coli* met-R2 couple $Fe^{III}_2/Fe^{II}Fe^{III}$ to be close to zero (see above) and k_{11} for the OR radicals to be 1.0×10^6 M^{-1} s^{-1},[19] the self-exchange rate constant k_{22} for the same couple is 7.6×10^5 M^{-1} s^{-1}.

Table 4. Rate Constants from Stopped-Flow Studies on the Reduction of the Active-R2 Component ($Fe^{III}_2\cdots Tyr^{\bullet}$) with Organic Radicals[a]

λ/nm	[parent]/ μM	[active-R2]/ μM	$10^{-5}k_1$[b]/ M^{-1} s^{-1}	$10^{-5}k_3$/ M^{-1} s^{-1}
		reaction of methylene blue		
660	4.5	30.8	7.5(2)	6.0(1)
660	7.4	30.8	7.2(3)	5.8(1)
660	9.9	46.7	7.3(3)	6.1(1)
		reaction of toluidine blue		
6.32	4.4	46.7	6.9(3)	5.7(2)
410	7.0(2)	5.9(2)		
632	6.6	30.8	6.8(2)	5.8(1)
632	9.1	30.8	6.8(3)	6.0(1)
		reaction of indo-phenol[c]		
603	4.1	30.8	0.11(1)	
603	5.8	30.8	0.11(1)	
410	0.10(2)			
604	8.1	46.7	0.13(1)	

[a] Solutions of the parent X were reduced with dithionite prior to stopped-flow studies. The program Glint was used to fit rate constants for active-R2 with $X^{\bullet}$ (k_1) and doubly reduced X^{2-} (k_3), with k_D fixed at 1.5×10^9 M^{-1} s^{-1}. [b] Listed as k_{12} in Table 5. [c] k_3 (and k_D) not relevant.

Table 5. Summary of Rate Constants k_{12} (22 °C) at pH 7.0 for the Reduction of Active- and Met-R2 from *E. coli* Ribonucleotide Reductase with Organic Radicals (OR) Determined by Pulse Radiolysis (PR) and Stopped-Flow (SF) Spectrophotometry[a]

OR	method (λ/nm)	E^o_1/V	log k_{12}	$-\log f$
		active-R2 as oxidant		
$MV^{\bullet+}$	PR(605)	−0.446	9.04	2.07
$BV^{\bullet+}$	PR(555)	−0.355	8.51	1.56
$Pf^{\bullet}$	PR(670)	−0.243	7.26	1.00
$Rb^{\bullet-}$	PR(550)	−0.200	7.04	0.76
Rf^{2-}	PR(700)	−0.059	6.43	0.25
$MB^{\bullet}$	SF(660)	+0.006	5.86[b]	0.115
$TB^{\bullet}$	SF(632)	+0.015	5.83[c]	0.115
$IP^{\bullet 2-}$	SF(603)	+0.194	4.04[d]	0.070
		met-R2 as oxidant		
$MV^{\bullet+}$	PR(606)	−0.446	9.28	2.07
$BV^{\bullet+}$	PR(555)	−0.355	8.53	1.56
$Pf^{\bullet}$	PR(670)	−0.243	7.52	1.00
$Rb^{\bullet-}$	PR(550)	−0.200	7.41	0.76
$Rf^{\bullet 2-}$	PR(700)	−0.059	6.54	0.25

[a] Reduction potentials E^o_1 vs NHE are for OR's. Values of log f were obtained from eq 3. [b] Less precise k_{12} value obtained by PR, 12.9×10^5 M^{-1} s^{-1}. [c] At 410 nm, $k_{12} = 7.0 \times 10^5$ M^{-1} s^{-1}. [d] At 410 nm, $k_{12} = 1.0 \times 10^4$ M^{-1} s^{-1}.

Discussion

With five OR's as reductants it was possible to determine rate constants for the reduction of active- and met-R2 forms by PR, Table 5. The coincidence of k_{12} values for the two forms, Figure 4, is significant since it indicates one-electron reduction of Fe^{III}_2 as rate limiting in both cases, with the $Tyr^{\bullet}$ of active-R2 playing a passive role. Subsequently, in the case of active-R2, the $Tyr^{\bullet}$ is reduced in an intramolecular step. Three other less reactive OR's ($MB^{\bullet}$, $TB^{\bullet}$, and $IP^{\bullet 2-}$) were studied by the

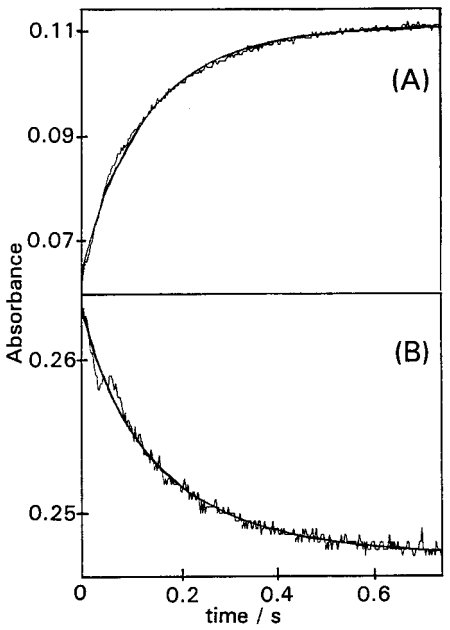

Figure 3. Fit of absorbance changes at (A) 632 and (B) 410 nm for the stopped-flow reduction of the *E. coli* active-R2 component (46.7 μM) with toluidine blue (4.9 μM), prior reduced with dithionite. Conditions: 22 °C, pH 7.0 (45 mM phosphate), I = 0.100 M.

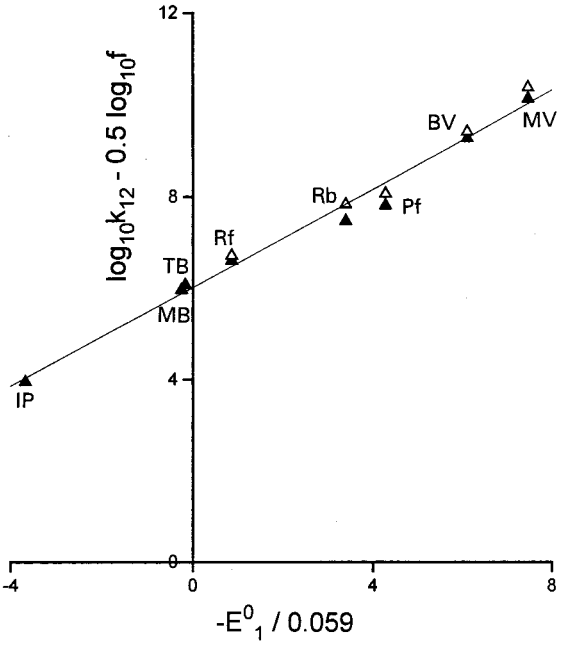

Figure 4. Marcus free-energy plot for reduction of active-R2 (▲) and met-R2 (△) from *E. coli* RNR by eight organic radicals (OR) as listed in Table 5. No reaction of met-R2 with MB•, TB•, and IP•2− is observed.

SF method, when only k_{12} values for reduction of active-R2 were obtained. With TB• and IP•2− the R2 absorbance decay at 410 nm gives identical rate constants to those obtained by monitoring re-formation of the parent, Figure 3. Absorption changes at 410 nm are bigger than those observed for the reduction of Fe^{III}_2 alone, and the differences are assigned to the decay of Tyr•. On this evidence it would appear that the rate of the Tyr• oxidation of $Fe^{II}Fe^{III}$ is comparable to the initial reduction of Fe^{III}_2.

No reduction of met-R2 is observed for the radicals MB•, TB•, or IP•2−, which have reduction potentials ≥0.011V, Table 5. Reduction of met-R2 with Rf•2− (−0.051 V) is observed, however. It is concluded that the reduction potential for the

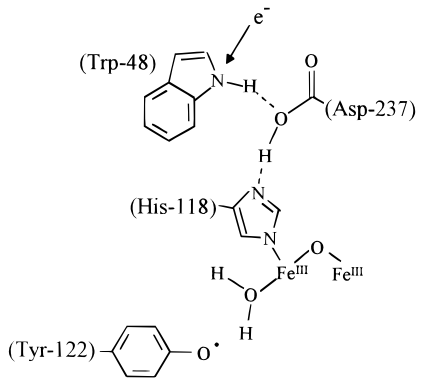

Figure 5. Pathway proposed for transfer of an electron from the indole ring of Trp-48 to His-118. A coordinated H_2O (for mouse[45]) or Asp-84[4] series as a contact to the phenolate O-atom of Tyr•.

$Fe^{III}_2/Fe^{II}Fe^{III}$ couple is between −0.051 and +0.011 V. The latter range is in keeping with an estimate of the mouse $Fe^{III}_2/Fe^{II}Fe^{III}$ couple of 0.010 to 0.150 V.[40] Since there is no reduction of met-R2 with MB•, TB•, and IP•2−, the mechanism of reduction of active-R2 has to be carefully considered. Formation of Fe^{II}-Fe^{III} followed by rapid reduction of Tyr• is able to explain the behavior observed. The latter does however need to be significantly faster than the reverse step involving $Fe^{II}Fe^{III}$ and the parent form.

The single linear Marcus correlation of rate constants for active- and met-R2, Figure 4, is in accordance with (4), and indicates a common rate-limiting electron-transfer (ET) process occurring between the OR (donor) and Fe^{III}_2 (acceptor) centers. However, the Tyr• is a much stronger oxidant (∼1.0 V),[39] and the exclusiveness of the Fe^{III}_2 step, with reduction of active and met-R2 occurring at similar rates, is an interesting outcome. A pathway for ET from Trp-48 at the surface of R2 via Asp-237 and His-118 (which is a ligand to Fe_A) has been proposed.[9] These amino acids are conserved,[5,41,42] and are connected by hydrogen bonds, Figure 5.[42,43] Variant *E. coli* and mouse R2 forms in which amino acids in the ET pathway are replaced by residues which are unable to H-bond severely impair redox activity.[42,43] Evidence has been presented that this pathway mediates electron transfer during O_2 activation.[44] Reduction of Tyr• may require a proton as well as an electron, in which case proton transfer involving the H-bonded chain between the donor and acceptor sites may be relevant by adaptation of Figure 5. Alternatively, the electron and proton may have other means of accessing the active site. For conversion through to red-R2 three electrons and three protons are required to retain electroneutrality at the active center.[45,46] Theoretical calculations have indicated unfavorable energetics for ET without the accompanying proton transfer to maintain electroneutrality.[46] Possible pathways for ET can be examined using the criteria of Beratan and Onuchic, and may involve atoms on the peptide backbone as well as the H-bonded route.[47,48] To initiate H^+ transfer in the present case a proton would have to be provided by solvent

(42) Persson, B. O.; Karlsson, M.; Climent, I.; Ling, J. S.; Loehr, J. S.; Sahlin, M.; Sjöberg, B.-M. *J. Biol. Inorg. Chem.* **1996**, *1*, 247.
(43) Katterle, B.; Sahlin, M.; Schmidt, P. P.; Pötsch, S.; Logan, D. T.; Gräslund, A.; Sjöberg, B.-M. *J. Biol. Chem.* **1997**, *272*, 10414.
(44) Parkin, S. E.; Chen, S.-X.; Ley, B. A.; Mangravite, L.; Edmondson, D. E.; Huynh, B. H.; Bollinger, J. M. *Biochemistry* **1998**, *37*, 1124−1130.
(45) Schmidt, P. P.; Rova, U.; Katterle, B.; Thelander, L.; Gräslund, A. *J. Biol. Chem.* **1998**, *273*, 21463.
(46) Siegbahn, P. E. M.; Blomberg, M. R. A.; Crabtree, R. H. *Theor. Chem. Acc.* **1997**, *97*, 289.
(47) Beratan, D. N.; Onuchic, J. N. *Photosynth. Res.* **1989**, *22*, 173.
(48) Beratan, D. N.; Onuchic, J. N.; Betts, J. N.; Bowler, B. E.; Gray, H. B. *J. Am. Chem. Soc.* **1990**, *112*, 7915.

H_2O rather than the reductant. Electron-transfer from the reductant OR to the Fe^{III}_2 site may drive the protonation step as in a similar instance involving redox coupled long-range proton transfer to the [3Fe-4S] cluster of *Azotobactor vinelandii*.[49] Interestingly, the Fe−S cluster is also buried and is inaccessible to solvent water.[50] A proton would thus travel to the binuclear iron acceptor site in what has been described as the "slipstream" of the electron.[49] Compliance with Marcus theory suggests that the rate controlling process is ET, and the similarity of rate constants for active and met-R2 indicates that ET terminates initially at Fe_A. In the case of *E. coli* R2, the chelated carboxylate of Asp-84 has been suggested as a possible mediator for proton transfer from the binuclear Fe to Tyr-122.[14]

The intercept at $-E^o_1/0.059 = 0$ in Figure 4 of 5.94 is equal to 0.5 ($\log k_{11} + \log k_{22} + E^o_2/0.059$), (4). The OR's are assumed to have a common self-exchange rate constant k_{11} of 1.0×10^6 M^{-1} s^{-1}, which gives an excellent correlation with cytochrome *c*(III) as oxidant.[19] As already discussed the reduction potential E^o_2 for the $Fe^{III}_2/Fe^{II}Fe^{III}$ couple has a value close to zero. Therefore the self-exchange rate constant k_{22} for the $Fe^{III}_2/Fe^{II}Fe^{III}$ exchange process is 7.6×10^5 M^{-1} s^{-1}, which is surprisingly favorable for a 10.9 Å (×2) separation of the binuclear Fe centers of two R2's. Larger E^o_1 values may be considered with k_{22} decreasing by an order of magnitude for each 0.059 V. The pathway for reduction of active- and met-R2 is only a part of the total enzyme requirement. When R1 and R2 associate, the pathway extends from Trp-48 via Tyr-356, Tyr-731, and Tyr-730 to Cys-438 at the substrate binding site of R1. The favorable self-exchange process k_{22} is relevant as a part of the communication between R1 and R2.

To summarize rate constants (k_{12}) for eight OR's, reduction potentials (E^o_1) in the range −0.446 to +0.194 V, as reductants for active- and met-R2, have been determined by PR and SF techniques. Rate constants for any one OR with active- and met-R2 forms are very similar (met on average 66% bigger), and reduction of the Fe^{III}_2 (E^o_2 close to zero) is rate controlling. A single linear free-energy plot of $\log k_{12}$ vs $E^o_1/0.059$ conforms to the Marcus equations, and ET is therefore the rate-controlling step. Reduction of the more strongly oxidizing adjacent $Tyr^•$ (reduction potential ∼1.0 V), in an overall process $Tyr^• + e^- + H^+ \rightarrow TyrH$, would serve to maintain electroneutrality of the buried active site. A reasonable hypothesis, but one which requires further examination, is that the electron and proton-transfer steps may occur via the conserved pathway from the surface Trp-48 to Asp-237, His-118, and Fe_A.

Acknowledgment. We are grateful for contributions to earlier parts of this work particularly from Drs. J.-Y Han and J.C. Swarts. Financial support was from the North of England Cancer Campaign, and UK Engineering and Physical Sciences Research Council. We also wish to acknowledge discussions with Professors A. Gräslund and J. M. Bollinger.

Supporting Information Available: Figures for fits of absorbance vs time data in PR experiments (PDF). This material is available free of charge via the Internet at http://pubs.acs.org.

JA993412K

(49) Hirst, J.; Duff, J. L. C.; Jameson, G. N. L.; Kemper, M. A.; Burgess, B. K.; Armstrong, F. A. *J. Am. Chem. Soc*. **1998**, *120*, 7085.

(50) It has also been proposed[49] that reoxidation of the $[3Fe\text{-}4S]^0H^+$ is controlled by the rate of release of the proton.